

Improved Analytical Delay Models for RC-Coupled Interconnects

Feng Shi, Xuebin Wu, and Zhiyuan Yan

Abstract—As the process technologies scale into deep sub-micron region, crosstalk delay is becoming increasingly severe, especially for global on-chip buses. To cope with this problem, accurate delay models of coupled interconnects are needed. In particular, delay models based on analytical approaches are desirable, because they not only are largely transparent to technology, but also explicitly establish the connections between delays of coupled interconnects and transition patterns, thereby enabling crosstalk alleviating techniques such as crosstalk avoidance codes (CACs). Unfortunately, existing analytical delay models, such as the widely cited model in [1], have limited accuracy and do not account for loading capacitance. In this paper, we propose analytical delay models for coupled interconnects that address these disadvantages. By accounting for more wires and eschewing the Elmore delay, our delay models achieve better accuracy than the model in [1].

Index Terms—Crosstalk, interconnect, delay, bus

I. INTRODUCTION

Crosstalk caused by coupling capacitance between adjacent wires leads to additional delay to multi-wire buses. As the process technologies scale into deep submicron region, coupling capacitance between adjacent wires and hence crosstalk delays increase greatly. According to the International Technology Roadmap of Semiconductors (ITRS) [2], gate delay **decreases** with scaling, while global wire delay **increases**. Hence, the crosstalk delay problem is becoming increasingly severe in VLSI designs, especially for global on-chip buses, and will become the performance bottleneck in many high-performance VLSI designs.

This paper focuses on analytical delay models applicable to general coupled interconnects. Although various delay models of interconnects have been proposed in the literature (see, for example, [1], [3]–[11]), few are comparable to our work in this paper. Some delay models (see, for example, [3]–[5], [7], [9], [11]) do not consider crosstalk from adjacent wires. Furthermore, most previously proposed delay models are based on numerical approaches (see, e.g., [3]–[5], [7]–[11]). They can achieve high accuracy, but they have several drawbacks. First, they sometimes lead to lookup tables of delays from any initial state to any next state (see, for example, [11]), which are often bulky and difficult to obtain and use. Second, numerical approaches in [3]–[5], [7], [9] are technology-dependent and their delays often depend on many parameters. Hence these approaches have poor portability and are not applicable to general cases. Third, the delays

obtained by the numerical approach offer little insight, and are not conducive to technology-independent crosstalk alleviation techniques such as crosstalk avoidance codes (CACs) (see, for example, [12]–[15]). Fourth, numerical approaches often have very high complexities. In contrast, analytical approaches are advantageous in these aspects. Analytical approaches depend on few technology parameters, and hence they are largely technology independent. Furthermore, analytical approaches illustrate the connection between delays of coupled interconnects and transition patterns, thus enabling us to design CACs. Finally, analytical approaches have very low computational complexities. A widely cited analytical delay model proposed by Sotiriadis *et al.* [1], [6], which uses the similar methodology to that in [16], appears to be the most comparable previous delay model to our work in this paper.

Based on the model in [1], [6], the delay of the k -th wire ($k \in \{1, 2, \dots, m\}$) of an m -bit bus is given by

$$T_k = \begin{cases} \tau_0[(1 + \lambda)\Delta_1^2 - \lambda\Delta_1\Delta_2], & k = 1 \\ \tau_0[(1 + 2\lambda)\Delta_k^2 - \lambda\Delta_k(\Delta_{k-1} + \Delta_{k+1})], & k \neq 1, m \\ \tau_0[(1 + \lambda)\Delta_m^2 - \lambda\Delta_m\Delta_{m-1}], & k = m, \end{cases} \quad (1)$$

where λ is the ratio of the coupling capacitance between adjacent wires and the ground capacitance of each wire, τ_0 is the intrinsic delay of a transition on a single wire, and Δ_k is 1 for $0 \rightarrow 1$ transition, -1 for $1 \rightarrow 0$ transition, or 0 for no transition on the k -th wire. We observe that in this model, the delay of the k -th wire depends on the transition patterns of wires $k-1$, k , and $k+1$ only. Since all possible values of T_k in Eq. (1) are $(1 + i\lambda)\tau_0$ for $i \in \{0, 1, 2, 3, 4\}$, all transition patterns on wires $k-1$, k , and $k+1$ can be divided into five classes according to their corresponding i . These five classes are denoted as iC for $i \in \{0, 1, 2, 3, 4\}$ (this classification was also used in [12]). Based on this model, various CACs (see, for example, [12]–[15]) have been proposed, based on the central idea of achieving a reduced delay by limiting transition patterns over the bus, at the expense of additional wires.

However, the model in [1] have two significant drawbacks. First, the model in [1] has limited accuracy. In a bus with more than three wires, the simulated wire delay for $0C$ transition patterns is much larger than τ_0 , the delay of $0C$ given by (1). This implies that the scheme that uses two shield wires with the same transition to achieve a delay of τ_0 (see, for example, [17]) will be ineffective. Our simulation results also show that the delays of other classes of transition patterns given by Eq. (1) have limited accuracy as well. This is partially because of the model's dependence on only three wires. Also, the model in [1] uses in its derivation the Elmore delay, which

Feng Shi, Xuebin Wu, and Zhiyuan Yan are with the Department of ECE, Lehigh University, PA 18015, USA. E-mails: {fes209, xuw207, yan}@lehigh.edu.

tends to overestimate the delay [18], [19].

The second drawback of the model in [1] is that it does not account for the loading capacitance. It has been shown that the loading capacitance is crucial in real practice and can affect the total delay for all patterns.

Addressing these disadvantages for the model in [1], in this paper we propose analytical delay models for coupled interconnects. Our delay models first derive closed-form expressions of the signals on the bus via a distributed RC model, and then approximate the wire delays by evaluating these closed-form expressions. Our delay models differ from the model in [1] in three aspects. First, in our delay models, we eschew the Elmore delay used in the model in [1]. Then, we consider either three wires or five wires in our delay models for improved accuracy. Due to these two differences, our models have significantly improved accuracy than the model in [1]. Finally, we take into account the buffer effects (driver resistance and loading capacitance). Our delay models also maintain the simplicity of the model in [1], and the transition patterns are divided into several categories based on their delays. Hence, our delay models are easy to use and conducive to the design of CACs. Although our delay models consider adjacent three and five wires in this paper, our models are applicable to buses of any number of wires.

Simulation results show that our delay models offer significant advantages than the model in [1]. Our simulations results fall into three scenarios. First, we compare the delays produced by our model and the model in [1] with the simulated delays for three- or five-wire buses. This is motivated by partial coding schemes (see, e.g., [12], [13], and [14]), which divide a wide bus into sub-buses with a few wires and separate them by shielding wires. Second, we obtain extensive simulation results for 17- and 33-wire buses assuming arbitrary transition patterns. Third, we assume the transition patterns are limited to those of CACs. In all three scenarios, our five-wire delay model is much more accurate than the model in [1].

With the scaling of technologies, the inductance is becoming significant and impacts the signals on the bus greatly. Due to the coupling effect of inductance, the worst-case patterns for an RLC modeled bus are quite different from that of an RC modeled bus [10]. Hence, the CAC design methodology would change greatly due to the inductance effect. However, our delay models do not consider the inductance effect for two reasons. First, it seems difficult to derive a closed-form expression of the signals on the bus based on the RLC model. Hence, our methodology cannot be easily adapted from the distributed RC model to an RLC model. Second, according to the criteria in [22], the inductance effect is significant in some cases, but are negligible in other cases. Specifically, the range of significance of the inductance effect is given by $\frac{t_r}{2\sqrt{lc}} < x < \frac{2}{r}\sqrt{\frac{l}{c}}$ [22], where x is the length of the wire, t_r the input transition time, and r , l , and c the resistance, inductance, and capacitance per unit length, respectively. According to [23], the inductance effect is not negligible for very deep submicron technologies and extremely long wires. In current industry applications, the on-chip inductance effect is still insignificant. This conclusion was also confirmed by other works: the 16-bit, 32Gb/s, 5mm-

long bus and 8-bit, 16Gb/s, 10mm-long bus in [24] show that the distributed RC model is sufficiently accurate for these high-speed long interconnects. In our work, our delay models are derived based on 5mm-long buses under a 45nm technology, where inductance effect is negligible.

The rest of the paper is organized as follows. In Section II, we propose our delay models. The delay models are also modified to account for the buffer effects. In Section III, we present extensive simulation results for our delay models. Concluding remarks are provided in Section IV.

II. DELAY MODEL

In this section, we first present the system model, where switching instants of all wires in the bus are assumed simultaneous. For three-wire and five-wire buses, we then derive closed-form expressions for outputs of the bus, and finally approximate their delays and compare them with those by the model in [1].

A. System model

In this paper, we focus on global interconnects connecting different modules for communication, such as data and address buses, and use the distributed RC model for interconnect modeling. For simplicity, we assume regular interconnects, which have uniformly distributed parameters and are paralleled routed in the same metal layer without turnings. Hence, the interconnects are modeled as transmission lines, which can be characterized by the telegrapher's equations. For complex interconnect structures with jumps and turnings, additional resistance due to vias and unequal length of wires should be included, which makes the interconnect behavior more complicated. However, crosstalk delays are expected to increase due to the additional resistance. The partially coupled buses are more complex and hence are not considered in this paper. We plan to investigate this in our future work. The capacitance between non-adjacent wires is negligible compared with capacitance between adjacent wires, since the capacitive coupling effect is a short range effect [16]. The distributed RC model is often used to approximate the buses [25]. Although the closed-form expressions of the signals on the bus via a distributed RC model are sums of infinite terms, usually sums of the two most significant terms provide a very close approximation of signals on the bus [26].

The distributed RC model of an m -wire bus is shown in Fig. 1, where $V_i(x, t)$ denotes the transient signal at a position x along wire i for $i \in \{1, 2, \dots, m\}$, r and c denote the resistance and capacitance per unit length, respectively. Also, λ_c denotes the coupling capacitance per unit length between two adjacent wires. The output resistance of a driver is approximated as a linear resistor, R_S , and the loading due to a receiver is modeled as a capacitance, C_L . In this work, we focus on a uniformly distributed bus and hence assume the parameters r , c , and λ are the same for all the wires.

We use the 50% delay, which is defined as the time difference between the respective instants when the input signal and corresponding output signal cross 50% of the supply voltage V_{dd} . According to [27], the delays of global interconnects are

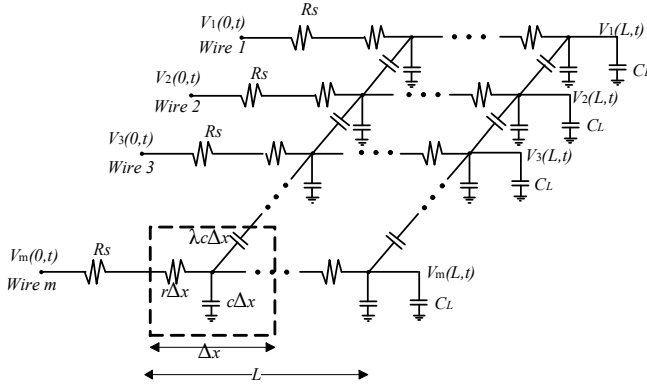


Fig. 1. A distributed RC model of an m -wire bus.

slightly affected by the slew rate. Since this work focuses on global interconnects, we ignore input slew and assume ideal step signals are applied on the bus directly. In this paper, we use the same classification iC for $i = 0, 1, 2, 3, 4$ in [1] and focus on the worst 50% delay of any wire for all classes to formulate our delay models. We consider the closest neighbors for crosstalk, since farther wires have weaker coupling effects. In Section II-B, we first focus on internal wire, wire 2 in a three-wire model, to account for most adjacent two wires (one wire to the left and one to the right). In Section II-C, we focus on internal wire, wire 3 in a five-wire model, to account for most adjacent four wires (two wires to the left and two to the right). In Section II-D, we derive the delay for boundary wires, wires 1, 2, 4, and 5 in a five-wire model. In Section II-F, we show how to identify the worst-case delays among all wires for a wide bus via a shift window scheme.

In this section, we first derive delay models by assuming that the buffer effects (driver resistance and loading capacitance) are negligible. This is an important case since the propagation delay is characterized only by the distributed interconnects. Then, in Section II-E, we modify the delay models to account for the buffer effects, which are crucial in real practice. It has been shown that the buffer effects would increase the total delay for all patterns.

Below we first investigate the case $m = 3$ and then extend our results to the case $m = 5$. There are two reasons for studying the three-wire model. First and foremost, the derivation of our five-wire model is based on the three-wire model. Second, our three-wire model is more accurate than our five-wire model for buses with only three wires, which is of interest for partial coding schemes (see, e.g., [12], [13], and [14]). We use T_m^{iC} to denote the worst delay of the middle wire (wire $\frac{m+1}{2}$) of an m -wire bus for all iC patterns.

B. Internal wires for three-wire model

In [26], the crosstalk of two coupled lines was described by partial differential equations (PDEs), and a technique for decoupling these highly coupled PDEs was introduced by using eigenvalues and corresponding eigenvectors. Using the same technique as in [26], we obtain the differential equations

describing a three-wire bus with length L :

$$\frac{\partial^2}{\partial x^2} \mathbf{V}(x, t) = \mathbf{RC} \frac{\partial}{\partial t} \mathbf{V}(x, t), \quad (2)$$

where $\mathbf{V}(x, t) = [V_1(x, t) \ V_2(x, t) \ V_3(x, t)]^T$ and $V_i(x, t)$ denotes the voltage of wire i at distance x ($0 \leq x \leq L$) at time t for $i = 1, 2, 3$, $\mathbf{R} = \text{diag}\{r \ r \ r\}$, and $\mathbf{C} = c \begin{bmatrix} 1 + \lambda & -\lambda & 0 \\ -\lambda & 1 + 2\lambda & -\lambda \\ 0 & -\lambda & 1 + \lambda \end{bmatrix}$.

The boundary conditions are given by

$$\begin{cases} V_i(0, t) = V_i^p - (V_i^p - V_i^f)u(t) & \text{for } i = 1, 2, 3 \\ I_i(L, t) = 0 \end{cases}$$

where V_i^p and V_i^f denote the initial and final voltages of the transition on wire i , respectively.

We find the three eigenvalues of \mathbf{C}/c , $p_1 = 1$, $p_2 = (1 + \lambda)$, and $p_3 = (1 + 3\lambda)$, and their corresponding eigenvectors \mathbf{e}_i 's, $[1 \ 1 \ 1]^T$, $[1 \ 0 \ -1]^T$, and $[-1 \ 2 \ -1]^T$, respectively. Hence, Eq. (2) is transformed to

$$\frac{\partial^2}{\partial x^2} U_i(x, t) = rcp_i \frac{\partial}{\partial t} U_i(x, t) \text{ for } i = 1, 2, 3, \quad (3)$$

where $U_i(x, t) = \mathbf{V}^T(x, t)\mathbf{e}_i$ for $i = 1, 2, 3$. So $U_1(x, t) = V_1(x, t) + V_2(x, t) + V_3(x, t)$, $U_2(x, t) = V_1(x, t) - V_3(x, t)$, and $U_3(x, t) = 2V_2(x, t) - V_1(x, t) - V_3(x, t)$.

Applying Laplace transform on both sides of Eq. (3), we have

$$\frac{\partial^2}{\partial x^2} U_i(x, s) = rcp_i [sU_i(x, s) - U_i(x, 0)] \text{ for } i = 1, 2, 3. \quad (4)$$

Using appropriate initial conditions, we solve Eq. (4) for $U_i(x, t)$ and obtain $V_2(L, t) = \frac{1}{3}[U_1(L, t) + U_3(L, t)]$. By solving $V_2(L, t) = 0.5V_{dd}$, we can approximate the 50% delay of a three-wire bus for different transition patterns.

In this paper, we use “ \uparrow ” to denote a transition from 0 to the supply voltage V_{dd} (normalized to 1), “ $-$ ” no transition, and “ \downarrow ” a transition from V_{dd} to 0.

For $0C$ pattern $\uparrow\uparrow\uparrow$, the output of wire 2 is given by [26] $V_2(L, t) = 1 + \sum_{n=1}^{\infty} \frac{(-1)^n}{\frac{\pi}{4}(2n-1)} e^{-\frac{t}{\tau}(2n-1)^2}$, where $\tau_0 = \frac{rcL^2}{2}$, and $\tau = \frac{8}{\pi^2}\tau_0$.

For the 50% delay, keeping only the first exponential term is accurate enough. So we have $V_2(L, t) \doteq 1 - \frac{4}{\pi}e^{-\frac{t}{\tau}}$. Similarly, we keep only the first exponential term as the solution for other cases. Solving $V_2(L, t) = 0.5$, we have $T_3^{0C} \doteq (\ln \frac{8}{\pi})\tau$. Similarly, the closed-form expressions of wire 2 and approximate delays for other classes are derived and summarized in Table I, where T_3^{iC} the approximate delay for iC pattern by our three-wire model.

C. Internal wires for five-wire model

To further improve the accuracy of delay, we include two extra adjacent wires to approximate the delay by considering the influences of all five wires. Each wire has three kinds of transition: \uparrow , $-$, and \downarrow . Hence, for such a five-wire bus, there are 3^5 transition patterns. To maintain the simplicity of our models, we still divide them into five classes (iC , $i \in \{0, 1, 2, 3, 4\}$) based on the transition patterns of middle three

TABLE I

CLOSED-FORM EXPRESSIONS OF SIGNAL ON WIRE 2 AND APPROXIMATE DELAYS IN A THREE-WIRE BUS ($V_2(L, t) = 1 - A_1 e^{-\frac{t}{\tau}} - A_2 e^{-\frac{t}{(1+3\lambda)\tau}}$, $\tau_0 = \frac{r_e L^2}{2}$, AND $\tau = \frac{8}{\pi^2} \tau_0$.)

iC	Worst Pattern	Coeffs. of $V_2(L, t)$		T_3^{iC}
		A_1	A_2	
0C	↑↑↑	$\frac{4}{\pi}$	0	$(\ln \frac{8}{\pi}) \tau$
1C	↑↑	$\frac{8}{3\pi}$	$\frac{4}{3\pi}$	$(\ln \frac{16}{\pi}) \tau$
2C	↑	$\frac{4}{3\pi}$	$\frac{8}{3\pi}$	$(\ln \frac{16}{3\pi}) (1 + 3\lambda) \tau$
3C	↓↑	0	$\frac{4}{\pi}$	$(\ln \frac{8}{\pi}) (1 + 3\lambda) \tau$
4C	↓↓	$-\frac{4}{3\pi}$	$\frac{16}{3\pi}$	$(\ln \frac{32}{3\pi}) (1 + 3\lambda) \tau$

wires (wires 2, 3, and 4). Hence, there are nine different transition patterns for each pattern of the same class.

Since the interconnect is a linear system, any pattern can be decomposed into a combination of patterns with transitions on a single wire. For example, ↑↑↓ is decomposed as (↑ - -) + (-↑ - -) + (- -↑ -) + (- - -↓). The delay expression of the middle wire impacted by any pattern is given by a summation of effects of individual wires on the middle wire. However, this approach would result in expressions that are hard to analyze. Instead, we propose to group these individual wires to form some special patterns, which can be analyzed easily.

Definition 1: Reducible transition pattern (RTP)

An RTP in the five-wire model is defined as a transition pattern that can be reduced to a transition pattern in the three-wire model. The set {↑↑↑↑, ↓↓↓↓, ↓↑↓, ↑↓↑} is the set of RTPs for the five-wire model.

For the transition ↑↑↑↑ (similarly for ↓↓↓↓), all wires have the same transitions. There are no coupling capacitance between any two adjacent wires. So the expression of wire 3 is approximated by $V_3(L, t) \doteq 1 - \frac{4}{\pi} e^{-\frac{t}{\tau}}$ and the delay is approximated by $(\ln \frac{8}{\pi}) \tau$. For the transition ↓↑↓ (similarly for ↑↓↑), wires 2 and 4 can be approximated as ground wires in the five-wire bus, since wire 1 (or 5) and wire 3 have opposite transitions. For wire 3, the five-wire pattern is equivalent to a three-wire pattern ↓↑↓, where the equivalent coupling capacitor between wire 1 (or 5) and wire 3 is equal to two capacitors in series between wires 1 and 2, and wires 2 and 3 (or wires 3 and 4, and wires 4 and 5). Hence, the equivalent coupling factor between wire 1 (or 5) and wire 3 is approximated as $\frac{\lambda}{2}$ per unit length (that is, the ratio of the coupling capacitance and the loading capacitance is $\frac{\lambda}{2}$). The expression of wire 3 is approximated by $V_3(L, t) \doteq 1 + \frac{4}{3\pi} e^{-\frac{t}{\tau}} - \frac{16}{3\pi} e^{-\frac{t}{(1+\frac{\lambda}{2})\tau}}$, and the delay is approximated by $\ln(\frac{16}{3\pi})(1 + \frac{\lambda}{2})\tau$.

Definition 2: Single transition pattern (STP)

An STP is defined to be a transition pattern with transitions on only one wire. For our five-wire model, we focus on the set of STPs with transitions on wire 2 or 4, {↑ - - -, -↓ - - -, - -↑ -, - - -↓}.

The expressions of wire 3 can be approximated by considering wires 2, 3, and 4 as a three-wire model. Let

TABLE II

DECOMPOSITION OF WORST-CASE PATTERNS IN THE FIVE-WIRE MODEL.

iC	Worst pattern	Decomposition
0C	↓↑↑↑↓	(↓↑↓)+(↑ - -)+(- -↑)
1C	↓↑↑↓	(↓↑↓)+(- -↑)
2C	↓↑↓	(↓↑↓)
3C	↑↓↑↑	(↑↑↑↑)+(- -↓)+(- -↓)+(-↓ - -)
4C	↑↓↑↓	(↑↑↑↑)+(↑↓ - -)+(↑↓ - -)+(-↓ - -)+(- -↓)

TABLE III

CLOSED-FORM EXPRESSIONS OF SIGNAL ON WIRE 3 AND APPROXIMATE DELAYS IN A FIVE-WIRE BUS

($V_3(L, t) = 1 - A_3 e^{-\frac{t}{\tau}} - A_4 e^{-\frac{t}{(1+\frac{\lambda}{2})\tau}} - A_5 e^{-\frac{t}{(1+3\lambda)\tau}}$, $\tau_0 = \frac{r_e L^2}{2}$, AND $\tau = \frac{8}{\pi^2} \tau_0$.)

iC	Worst Pattern	Coeffs. of $V_3(L, t)$			T_5^{iC}
		A_3	A_4	A_5	
0C	↓↑↑↑↓	$\frac{4}{3\pi}$	$\frac{16}{3\pi}$	$-\frac{8}{3\pi}$	$0.165(1 + 3\lambda)\tau$
1C	↓↑↑↓	0	$\frac{16}{3\pi}$	$-\frac{4}{3\pi}$	$0.384(1 + 3\lambda)\tau$
2C	↓↑↓	$-\frac{4}{3\pi}$	$\frac{16}{3\pi}$	0	$(\ln \frac{32}{3\pi}) (1 + \frac{\lambda}{2})\tau$
3C	↑↓↑↑	0	0	$\frac{4}{\pi}$	$(\ln \frac{8}{\pi}) (1 + 3\lambda)\tau$
4C	↑↓↑↓	$-\frac{4}{3\pi}$	0	$\frac{16}{3\pi}$	$(\ln \frac{32}{3\pi}) (1 + 3\lambda)\tau$

$V_j^i(x, t)$ denote the signal on wire j due to coupling from wire i . For example, by ignoring coupling from wires 1 and 5 in ↑ - -, the output of wire 3 is approximated by $V_3^2(L, t) \doteq -\frac{4}{3\pi} e^{-\frac{t}{\tau}} + \frac{4}{3\pi} e^{-\frac{t}{(1+3\lambda)\tau}}$, which is obtained by considering only wires 2, 3, and 4.

We propose the following approaches to derive the delay of the five-wire bus.

- We first **decompose** the worst pattern in each class into a combination of an RTP and STP(s).
- Then we combine the expressions of the RTP and STP(s) for the middle wire based on the conclusion of our three-wire model.
- Finally, we evaluate the expression of the middle wire to approximate its delay.

Since the performance is limited by the worst-case delay in each class, we need to approximate the delays of only the worst patterns in each class. We use simulation to identify the worst patterns in all classes. The worst patterns for 0C to 4C are given by ↓↑↑↑↓, ↓↑↑↓, ↓↑↓, ↑↓↑↑, and ↑↓↑↓, respectively (assuming the middle wire has an upward transition). With RTPs and STPs, we decompose the worst pattern in each class as shown in Table II.

The closed-form expressions of wire 3 and approximate delays for all classes in a five-wire bus are derived and summarized in Table III, where T_5^{iC} the approximate delay for iC pattern by our three-wire model.

D. Boundary wires

In the previous derivation, we focus on middle wires and consider four neighboring wires (two to the left and two to the right) for crosstalk. In this section, we derive delay models to account for the boundary wires of an m -wire bus (wires 1, 2, $m-1$, and m). For wire 1 (wire m), we consider wires 2 and 3

TABLE IV

CLOSED-FORM EXPRESSIONS OF SIGNAL ON WIRE 1 AND APPROXIMATE DELAYS ($V_1(L, t) = 1 - A_6 e^{-\frac{t}{\tau}} - A_7 e^{-\frac{t}{(1+\lambda)\tau}} - A_8 e^{-\frac{t}{(1+3\lambda)\tau}}$, $\tau_0 = \frac{rcL^2}{2}$, AND $\tau = \frac{8}{\pi^2} \tau_0$.)

iC	Worst Pattern	Coeffs. of $V_1(L, t)$			T_{b1}^{iC}
		A_6	A_7	A_8	
0C	$\uparrow\uparrow\downarrow$	$\frac{4}{3\pi}$	$\frac{4}{\pi}$	$-\frac{4}{3\pi}$	$0.783(1+\lambda)\tau$
1C	$\uparrow\downarrow$	0	$\frac{4}{\pi}$	0	$(\ln \frac{8}{\pi})(1+\lambda)\tau$
2C	$\uparrow\downarrow\downarrow$	$-\frac{4}{3\pi}$	$\frac{4}{\pi}$	$\frac{4}{3\pi}$	$1.094(1+\lambda)\tau$

TABLE V

CLOSED-FORM EXPRESSIONS OF SIGNAL ON WIRE 2 AND APPROXIMATE DELAYS ($V_2(L, t) = 1 - A_9 e^{-\frac{t}{\tau}} - A_{10} e^{-\frac{t}{(1+2\lambda)\tau}} - A_{11} e^{-\frac{t}{(1+(2-\sqrt{2})\lambda)\tau}} - A_{12} e^{-\frac{t}{(1+(2+\sqrt{2})\lambda)\tau}}$, $\tau_0 = \frac{rcL^2}{2}$, AND $\tau = \frac{8}{\pi^2} \tau_0$.)

iC	Worst Pattern	Coeffs. of $V_2(L, t)$				T_{b2}^{iC}
		A_9	A_{10}	A_{11}	A_{12}	
0C	$\uparrow\uparrow\uparrow\downarrow$	$\frac{2}{\pi}$	$\frac{2}{\pi}$	$\frac{\sqrt{2}}{\pi}$	$-\frac{\sqrt{2}}{\pi}$	$(\ln \frac{8}{\pi})\tau$
1C	$-\uparrow\uparrow\downarrow$	$\frac{1}{\pi}$	$\frac{3}{\pi}$	$\frac{\sqrt{2}}{2\pi}$	$-\frac{\sqrt{2}}{2\pi}$	$0.427(1+2\lambda)\tau$
2C	$\downarrow\uparrow\uparrow\downarrow$	0	$\frac{1}{\pi}$	0	0	$(\ln \frac{8}{\pi})(1+2\lambda)\tau$
3C	$\downarrow\uparrow\uparrow$	$\frac{1}{\pi}$	$\frac{1}{\pi}$	$\frac{2-3\sqrt{2}}{2\pi}$	$\frac{2+3\sqrt{2}}{2\pi}$	$1.441(1+2\lambda)\tau$
4C	$\downarrow\uparrow\downarrow\uparrow$	0	0	$\frac{2(1-\sqrt{2})}{\pi}$	$\frac{2(1+\sqrt{2})}{\pi}$	$6.540(1+(2-\sqrt{2})\lambda)\tau$

to the right (wires $m-2$ and $m-1$ to the left) for crosstalk, and use the same classification as in Eq. (1) [1]. Note that for wires 1 and m , there are only three classes of patterns, 0C, 1C, and 2C. With the similar technique, the closed-form expressions of wire 1 (wire m) and approximate delays for all classes are derived and summarized in Table IV, where T_{b1}^{iC} is the approximate delay for iC pattern. For wire 2 (wire $m-1$), we consider wire 1 to the left and wires 3 and 4 to the right (wires $m-3$, $m-2$ to the left and wire m to the right) for crosstalk. Similarly, the closed-form expressions of wire 2 (wire $m-1$) and approximate delays for all classes are derived and summarized in Table V, where T_{b2}^{iC} is the approximate delay for iC pattern.

E. Revised models with consideration of the buffer effects

In the previous derivation, the buffer effects are ignored with assumption that the driver resistance and loading capacitance are relatively small. In practice, the values of resistance and capacitance vary with different structure of buffers. In this work, we consider drivers and receivers implemented as a non-inverting inverter chain. The simplest one has two chained inverters. The loading capacitance C_L and driver resistance R_S are due to the first and last stage inverters in the chain, respectively. The buffer strength is measured by the normalized size of inverter to the smallest inverter. For global interconnects in submicron technology, the loading capacitance is not significantly large in comparison with that of interconnect. According to [28], for a 45nm technology [29], the loading capacitance C_L induced by a 100 times inverter is given by 25 fF. In this paper, we consider loading capacitance as large as 100 fF. For significantly large C_L , the delay due to

TABLE VI

EXPRESSIONS OF MIDDLE WIRE IN A THREE-WIRE MODEL, WHERE $V_2(L, t) = 1 - b_1 B_1 e^{-\frac{t}{\tau_1}} - b_2 B_2 e^{-\frac{t}{\tau_2}}$, $B_1 = 1.01 \frac{R_T + C_T + 1}{R_T + C_T + \frac{1}{4}}$, $B_2 = 1.01 \frac{R_T + C_T^* + 1}{R_T + C_T^* + \frac{1}{4}}$, $\tau_1 = \frac{RC(R_T C_T + R_T + C_T + (\frac{2}{\pi})^2)}{1.04}$, $\tau_2 = \frac{(1+3\lambda)RC(R_T C_T^* + R_T + C_T^* + (\frac{2}{\pi})^2)}{1.04}$, $R_T = \frac{R_S}{R}$, $C_T = \frac{C_L}{C}$, $C_T^* = \frac{1.04}{(1+3\lambda)C}$, $C = cL$, AND $R = rL$.

iC	Worst Pattern	Coeffs. of $V_2(L, t)$		T_3^{iC}
		b_1	b_2	
0C	$\uparrow\uparrow\uparrow$	1	0	$(\ln 2B_1)\tau_1$
1C	$\uparrow\uparrow\downarrow$	$\frac{2}{3}$	$\frac{1}{3}$	$(\ln 4B_1)\tau_1$
2C	$-\uparrow\downarrow$	$\frac{1}{3}$	$\frac{2}{3}$	$(\ln \frac{4B_2}{3})\tau_2$
3C	$\downarrow\uparrow\downarrow$	0	1	$(\ln 2B_2)\tau_2$
4C	$\downarrow\uparrow\uparrow$	$-\frac{1}{3}$	$\frac{4}{3}$	$(\ln \frac{8B_2}{3})\tau_2$

TABLE VII

EXPRESSIONS OF MIDDLE WIRE IN A FIVE-WIRE MODEL, WHERE $V_3(L, t) = 1 - b_3 B_3 e^{-\frac{t}{\tau_1}} - b_4 B_4 e^{-\frac{t}{\tau_2}} - b_5 B_5 e^{-\frac{t}{\tau_3}}$, $B_3 = 1.01 \frac{R_T + C_T + 1}{R_T + C_T + \frac{1}{4}}$, $B_4 = 1.01 \frac{R_T + C_T^* + 1}{R_T + C_T^* + \frac{1}{4}}$, $B_5 = 1.01 \frac{R_T + C_T^\dagger + 1}{R_T + C_T^\dagger + \frac{1}{4}}$, $\tau_1 = \frac{RC(R_T C_T + R_T + C_T + (\frac{2}{\pi})^2)}{1.04}$, $\tau_2 = \frac{(1+\frac{3}{2}\lambda)RC(R_T C_T^* + R_T + C_T^* + (\frac{2}{\pi})^2)}{1.04}$, $\tau_3 = \frac{(1+3\lambda)RC(R_T C_T^\dagger + R_T + C_T^\dagger + (\frac{2}{\pi})^2)}{1.04}$, $R_T = \frac{R_S}{R}$, $C_T = \frac{C_L}{C}$, $C_T^* = \frac{C_L}{(1+\frac{3}{2}\lambda)C}$, $C_T^\dagger = \frac{C_L}{(1+3\lambda)C}$, $C = cL$, $R = rL$, $f_1 = (-\ln(\frac{1}{4} + \frac{1}{2}\sqrt{\frac{1}{4} + \frac{3}{2B_3}}))$, AND $f_2 = (-\ln(\frac{1}{8} + \frac{1}{2}\sqrt{\frac{1}{16} + \frac{3}{2B_5}}))$.

iC	Worst Pattern	Coeffs. of $V_3(L, t)$			T_5^{iC}
		b_3	b_4	b_5	
0C	$\downarrow\uparrow\uparrow\uparrow\downarrow$	$\frac{1}{3}$	$\frac{4}{3}$	$-\frac{2}{3}$	$f_1 \tau_3$
1C	$\downarrow\uparrow\uparrow\downarrow$	0	$\frac{4}{3}$	$-\frac{1}{3}$	$f_2 \tau_3$
2C	$\downarrow\uparrow\downarrow\downarrow$	$-\frac{1}{3}$	$\frac{4}{3}$	0	$(\ln \frac{8B_4}{3})\tau_2$
3C	$\uparrow\downarrow\uparrow\uparrow$	0	0	1	$(\ln 2B_5)\tau_3$
4C	$\uparrow\downarrow\uparrow\downarrow$	$-\frac{1}{3}$	0	$\frac{4}{3}$	$(\ln \frac{8B_5}{3})\tau_3$

C_L would dominate the total propagation delay and all classes of patterns would collapse into one class. In the following, we revise our models to capture the buffer effects of R_S and C_L at the inputs and outputs of the interconnects, respectively.

First, we focus on our three-wire model. With consideration of buffer effects, the differential equation is still given by Eq. (2). Only the boundary conditions need to be changed. The revised boundary conditions are given by

$$\begin{cases} V_i(0, t) = V_i^p - (V_i^p - V_i^f)u(t) - I_i(0, t)R_S \\ I_i(L, t) = C_L \frac{\partial}{\partial t} V_i(L, t) \end{cases} \quad \text{for } i = 1, 2, 3$$

By solving the differential equations of a three-wire bus, we derive the expressions of all worst-case patterns as shown in Table VI. The revised delay expressions are listed in column five of Table VI. Note that the revised three-wire delay model would reduce to that in Table I, when the driver resistance and loading capacitance are relatively small, $R_T \doteq 0$ and $C_T \doteq 0$.

Similarly, for a five-wire bus, we derive the expressions of all worst-case patterns in each class as shown in Table VII. The ratio between τ_2 and τ_3 is given by $\frac{\tau_2}{\tau_3} = \frac{(1+\frac{3}{2}\lambda)RC(R_T C_T^* + R_T + C_T^* + (\frac{2}{\pi})^2)}{(1+3\lambda)RC(R_T C_T^\dagger + R_T + C_T^\dagger + (\frac{2}{\pi})^2)} \doteq \frac{1}{2}$. Then the 50% delay can be solved by assuming $e^{-\frac{t}{\tau_2}} = (e^{-\frac{t}{\tau_3}})^2$. The revised

TABLE VIII
BUS PARAMETERS IN A 45nm TECHNOLOGY.

Parameters			
L	5 mm	r	13.75 Ω/mm
w	0.8 μm	l	1.736 nH/mm
s	0.8 μm	c	8.263 fF/mm
t	2 μm	c_c	101.136 fF/mm
h	4.82 μm	R_S	100 Ω
K_{ILD}	2.5	C_L	0 fF

delay expressions are listed in column six of Table VII. Note that the revised five-wire delay model would reduce to that in Table III, when the driver resistance and loading capacitance are relatively small, $R_T \doteq 0$ and $C_T \doteq 0$.

According to the delay expressions in Tables VI and VII, both driver resistance and loading capacitance tend to increase the delay. When the loading capacitance increases, the delay difference among all classes diminishes. For extremely large C_L , the delays for all classes are close and the classification becomes inconsequential.

F. Characterization of the delay of a multi-wire bus

In the derivation of our five-wire model above, we focus on the worst-case patterns of the middle wires only. We also derive delay models for boundary wires. In the following, we show that our five-wire model can be easily applied to approximate the delays of an m -wire bus ($m > 5$). First, we use our five-wire delay model as a shift window to scan the internal wires (wires 3 through $m - 2$) to identify the longest delay. Then, for boundary wires (wires 1, 2, $m - 1$, and m), we use the models in Tables IV and V for delay approximation. Hence, the delay of an m -wire bus is given by the largest delay among all wires. For example, for a pattern $\uparrow\downarrow\uparrow\downarrow\downarrow$ of a six-wire bus, the classes for wires 1 through 6 are given by $2C$, $4C$, $4C$, $2C$, $0C$, and $0C$, respectively. Thus, the worst-case class is given by $4C$. According to our models in Tables III, IV, and V, the worst-case delay is given by the larger one of the two delays $6.540(1 + (2 - \sqrt{2})\lambda)\tau$ and $(\ln \frac{32}{3\pi})(1 + 3\lambda)\tau$.

The proposed analytical delay models target two important applications. One primary application of our model is the design of crosstalk avoidance codes (CACs). Since our proposed models provide more accurate delays for different transition patterns than previous models, we can identify unwanted patterns more effectively. Second, our models can be applied to partial coding schemes, where buses are broken into sub-buses, since our models are more accurate for a bus of small size. To incorporate such analytical delay models in EDA softwares, such as a typical timing analysis flow, appropriate adjustments are needed. We plan to investigate this important scenario in our future work.

G. Discussion on synchronization problems

In previous subsections, we assume simultaneous transitions on all the wires. However, for global buses where buffer insertion techniques are usually used to reduce their delay [20], simultaneous signal transitions on the bus cannot be

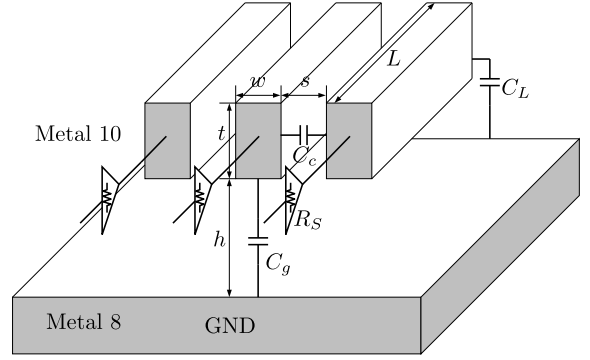


Fig. 2. Interconnect structure.

guaranteed. Our derived models do not work for buses with synchronization problems. In the following, we briefly discuss the synchronization problems and conclude with insights on the delay changes of interconnects with synchronization problems and impacts on the CAC designs.

Based on our three-wire and five-wire models, we observe **two possible scenarios** with regard to the impact of synchronization problems on the delay. When the time differences are relatively small, the delay is increased only by the time differences. When the time differences are sufficiently large, they can change the worst delay of a class to a different class. For instance, the delays of the transition patterns in $0C$ and $1C$ may be increased to those of $2C$ when the time differences are large enough, and similarly $2C$ to $3C$. This is consistent with the observation in [17]. On the other hand, the delays of the transition patterns in $3C$ may decrease to those of $2C$ class when the time differences are large enough. Intuitively, this is because large time differences change the intended transition patterns into different patterns. As observed above, depending on the severity of the synchronization problems, the effectiveness of CACs is affected to a varying extent. Furthermore, the sensitiveness to time differences varies with CACs.

III. PERFORMANCE EVALUATION

We evaluate the performance of our delay models, and compare it with that of the model in [1] in three scenarios. First, since our delay models focus on three and five adjacent wires, we consider three- and five-wire buses. This scenario is also motivated by partial coding schemes (see, e.g., [12], [13], and [14]), which divide a wide bus into sub-buses with a few wires and separate them by shielding wires. The second scenario is buses with more than five wires. We have run extensive simulations on buses with an odd number of wires (up to 33 wires). Our conclusions are the same regardless of the number of wires. For brevity, we present our simulation results for 17- and 33-wire buses. In the first two scenarios, we focus on the worst-case delays of the middle wires. To characterize the whole bus transitions, our five-wire model can be applied to all wires to approximate their delays with higher accuracy. In the third scenario, we assume the transition patterns are limited to those of CACs and consider the worst-case delays for all wires of an 8-wire bus.

TABLE IX

COMPARISON OF SIMULATED DELAYS, DELAYS OF OUR THREE-WIRE MODEL AND THE MODEL IN [1]. ALL THE DELAYS ARE IN ps.

iC	Worst pattern	Sim.	Our model		[1]	
		T_d	T_3^{iC}	$\frac{ T_3^{iC}-T_d }{T_d}$	T_2	$\frac{ T_2-T_d }{T_d}$
0C	↑↑↑	3.96	4.04	2.02%	5.55	40.15%
1C	↑↑-	7.41	7.56	2.02%	73.50	891.90%
2C	-↑-	72.28	74.55	3.14%	141.45	95.70%
3C	↓↑-	150.74	152.24	1.00%	209.40	38.91%
4C	↓↑↓	206.40	207.36	0.47%	277.35	34.38%

All the simulation results in this paper are obtained by the following setup. The simulation is based on a 45nm technology with 10 metal layers [29]. The global buses are routed in the top two metal layers, 10 and 9, with a ground metal layer 8 down below as shown in Fig. 2. We consider metal layer 10 for all buses, since the crosstalk is more serious than that of metal layer 9. The bus parameters are obtained by structure 1 in [30] and summarized in Table VIII, where K_{ILD} is the permittivity of the dielectric between metals. Since the model in [1] does not account for the loading capacitance, we assume $C_L = 0$ fF for simulations in comparison with the model in [1]. We also simulate 17- and 33-wire buses with $C_L = 100$ fF, which represents the loading capacitance induced by a 400 times inverter. The coupling factor is given by $\lambda = \frac{c_v}{c} \doteq 12.2$. For inputs with $t_r = 10$ ps, inductance effect is negligible when $1.3 \text{ mm} < L < 66.7 \text{ mm}$. All the buses for simulation have a length of 5 mm and the inductance effect is not considered in this work. The buses are divided into 100 sections as shown in Fig. 1 to characterize the distributed RC model. The simulation results are obtained from HSPICE.

A. Three-wire and five-wire buses

For a three-wire bus, the simulated delays are compared with the delays by our model and the model in [1] for all classes in Table IX, where T_d denotes the simulated worst delay of wire 2, T_3^{iC} the approximate delay for iC pattern by our three-wire model, and T_2 by the model in [1]. The error percentages of our model and the model in [1] are also shown in Table IX. For all five classes of transition patterns, the **maximum** and **minimum** errors by our model are only 3.14% and 0.47%, respectively, as opposed to 891.90% and 34.38% by the model in [1], respectively. As Table IX shows, our model is much more accurate than the model in [1] for all patterns in a three-wire bus. We remark that the delay by our model for the 1C pattern, $(\ln \frac{16}{\pi}) \tau$, does not depend on λ .

For a five-wire bus, the worst delays of all classes of transition patterns based on our five-wire model are compared with those of the model in [1] as well as the simulated delays by HSPICE in Table X, where T_d denotes the simulated worst-case delay of wire 3 for all iC patterns, T_5^{iC} the approximate delay for iC pattern by our five-wire model, and T_3 by the model in [1]. The error percentages of our model and the model in [1] are shown in Table X. For a five-wire bus the **maximum** and **minimum** errors by our model are 34.41% and 1.59%, respectively, in comparison to 84.28% and 16.50% by

TABLE X

COMPARISON OF SIMULATED DELAYS, DELAYS OF OUR FIVE-WIRE MODEL AND THE MODEL IN [1]. ALL THE DELAYS ARE IN ps.

iC	Worst pattern	Sim.	Our model		[1]	
		T_d	T_5^{iC}	$\frac{ T_5^{iC}-T_d }{T_d}$	T_3	$\frac{ T_3-T_d }{T_d}$
0C	↓↑↑↑↓	35.30	23.15	34.41%	5.55	84.28%
1C	↓↑↑↓	63.09	62.09	1.59%	73.50	16.50%
2C	↓↑↑↓	98.39	106.43	8.17%	141.45	43.76%
3C	↑↑↑↑↑	134.19	152.24	13.45%	209.40	56.05%
4C	↑↑↑↑↑	218.91	207.36	5.28%	277.35	26.70%

the model in [1], respectively. As Table X shows, our five-wire model is more accurate than the model in [1] for all patterns in a five-wire bus. In particular, although the delays in the model in [1] were claimed to be upper bounds on the actual delays, our simulation results in Table X show that this claim is invalid for the 0C patterns. In [17], the author proposed a method which achieves a delay of τ_0 by surrounding each data wire with two shield wires with the same transition. Since the transition patterns for each data wire are always in 0C class, the delays of the data wires are τ_0 according to the model in [1]. In contrast, the delay for the data wires can be as large as $0.165(1+3\lambda)\tau_0$ by our model; When λ is large, the model in [1] severely underestimates the delay, while our model is more accurate.

B. 17-wire and 33-wire buses

We next compare our five-wire model with the model in [1] for 17- and 33-wire buses. With a 17-wire bus, we focus on the middle wire (wire 9). We still classify the transition patterns according to the transitions of the middle three wires (wires 8, 9, and 10). Since it is time consuming to identify the transition patterns with the longest delay in each class, we make one assumption about the patterns with the longest delay in each class. For any two wires symmetric to wire 9 (wire i and wire $18-i$, $i \in \{1, 2, \dots, 8\}$), there are nine possible patterns, $\uparrow\uparrow$, $\downarrow\downarrow$, $-$, $\uparrow-$, $-\uparrow$, $\downarrow-$, $-\downarrow$, $\uparrow\downarrow$, and $\downarrow\uparrow$. For patterns in opposite direction, we assume the influences of the two wires will cancel out because of symmetry. For other patterns, if the upward transition of one wire increases the delay, we see that $\uparrow\uparrow$ has greater delay than $\uparrow-$ or $-\uparrow$. Similarly, if the downward transition increases the delay, the pattern $\downarrow\downarrow$ has greater delay than $\downarrow-$ or $-\downarrow$. So we assume that the longest delay happens when two symmetric wires have either $\uparrow\uparrow$ or $\downarrow\downarrow$ transitions.

Based on this assumption, we search all possible symmetric transition patterns to find the worst-case patterns in each class, which are listed in the second column of Table XI, where the pattern on wires 8, 9, and 10 are shown in the parenthesis. The simulated worst-case delays for all iC , denoted by T_d , are compared with the delays by our five-wire model and the model in [1] in Table XI. The error percentage of our model and the model in [1] are also shown in Table XI. For all five classes, the **maximum** and **minimum** errors by our model are only 45.10% and 5.66%, respectively, as opposed to 86.84% and 8.89% by the model in [1], respectively. For all classes except 1C, our five-wire model outperforms the model in [1]. The model in [1] also has a large error percentage for 0C.

TABLE XI

COMPARISON OF SIMULATED DELAYS AND DELAYS GIVEN BY OUR FIVE-WIRE MODEL AND THE MODEL IN [1] FOR WIRE 9 IN A 17-WIRE BUS WITH $C_L = 0$ fF. ALL THE DELAYS ARE IN ps.

iC	Worst patterns via Alg. 1	Sim.	Our model			[1]
		T_d	T_5^{iC}	$\frac{ T_5^{iC} - T_d }{T_d}$	T_9	$\frac{ T_9 - T_d }{T_d}$
0C	↑↑↑↑↓↓ (↑↑↑) ↓↓↑↑↑↑	42.17	23.15	45.10%	5.55	86.84%
1C	↑↑↑↑↓↓ (↑↑ -) ↓↓↑↑↑↑	67.50	62.09	8.01%	73.50	8.89%
2C	↓↑↑↑↑↓ (-↑ -) ↓↑↑↑↑↓	112.82	106.43	5.66%	141.45	25.38%
3C	↓↑↑↑↑↓ (↓↑ -) ↓↑↑↑↑↓	165.44	152.24	7.98%	209.40	26.57%
4C	↑↓↑↑↑↑ (↓↑) ↑↑↑↓↑↑	228.46	207.36	9.24%	277.35	21.40%

TABLE XII

COMPARISON OF SIMULATED DELAYS AND DELAYS GIVEN BY OUR FIVE-WIRE MODEL AND [1] FOR WIRE 17 IN A 33-WIRE BUS WITH $C_L = 0$ fF. ALL THE DELAYS ARE IN ps.

iC	Worst patterns via Alg. 1	Sim.	Our model			[1]
		T_d	T_5^{iC}	$\frac{ T_5^{iC} - T_d }{T_d}$	T_{17}	$\frac{ T_{17} - T_d }{T_d}$
0C	↓↓↑↑↑↑↑↑↑↑ (↑↑↑) ↓↓↑↑↑↑↑↑↑↑	42.27	23.15	45.23%	5.55	86.87%
1C	↓↓↑↑↑↑↑↑↑↑ (-↑↑) ↓↓↑↑↑↑↑↑↑↑	68.30	62.09	9.09%	73.50	7.61%
2C	↑↑↑↑↑↑↑↑↑↑ (-↑ -) ↓↑↑↑↑↑↑↑↑↑	113.16	106.43	5.95%	141.45	25.00%
3C	↓↑↑↑↑↑↑↑↑↑ (-↑↓) ↓↑↑↑↑↑↑↑↑↑	165.57	152.24	8.05%	209.40	26.47%
4C	↓↑↑↑↑↑↑↑↑↑ (↓↑) ↑↑↑↓↑↑↑↑↑↑	229.02	207.36	9.46%	277.35	21.10%

TABLE XIII

COMPARISON OF SIMULATED DELAYS AND DELAYS GIVEN BY OUR FIVE-WIRE MODEL FOCUSING ON THE MIDDLE WIRE IN A 17-WIRE AND A 33-WIRE BUSES WITH $C_L = 100$ fF. ALL THE DELAYS ARE IN ps.

iC	Worst 17-wire patterns via Alg. 1	Sim.	Our model			Worst 33-wire patterns via Alg. 1	Sim.	Our model		
		T_d	T_5^{iC}	$\frac{ T_5^{iC} - T_d }{T_d}$			T_d	T_5^{iC}	$\frac{ T_5^{iC} - T_d }{T_d}$	
0C	↑↑↑↑↓↓ (↑↑↑) ↓↓↑↑↑↑	50.75	25.11	50.52%		↓↓↑↑↑↑↑↑↑↑ (↑↑↑) ↓↓↑↑↑↑↑↑↑↑	50.78	25.11	50.55%	
1C	↑↑↑↑↓↓ (↑↑ -) ↓↓↑↑↑↑	76.42	67.35	11.87%		↓↓↑↑↑↑↑↑↑↑ (-↑↑) ↓↓↑↑↑↑↑↑↑↑	76.43	67.35	11.88%	
2C	↑↑↑↑↑↓ (-↑ -) ↓↑↑↑↑↑	118.92	123.46	3.82%		↑↑↑↑↑↑↑↑↑↑ (-↑ -) ↓↑↑↑↑↑↑↑↑↑	119.21	123.46	3.57%	
3C	↓↑↑↑↑↓ (↓↑ -) ↓↑↑↑↑↓	177.71	164.62	7.37%		↓↑↑↑↑↑↑↑↑↑ (-↑↓) ↓↑↑↑↑↑↑↑↑↑	177.74	164.62	7.38%	
4C	↑↓↑↑↑↑ (↓↑) ↑↑↑↓↑↑	236.18	224.41	4.98%		↓↑↑↑↑↑↓↑↑↑↑↑ (↓↑) ↑↑↑↓↑↑↑↑↑↑	236.67	224.41	5.18%	

With a 33-wire bus, we focus on the delay of the middle wire (wire 17). Since there are 3^{33} transition patterns, it is infeasible to search all possible symmetric transitions as before to find the worst-case patterns. We make the following three assumptions: (1) The worst patterns in each classes are symmetric; (2) The closer the wire gets to the middle wire, the greater the coupling on the settling of the middle wire; (3) We initialize the middle three wires to a pattern in iC , and initialize all other wires with opposite transitions to the middle wire. Based on these three assumptions, we use Alg. 1 to find the patterns with largest delays. We denote by P_i the updated transition pattern of an m -wire bus after the i -th iteration of Alg. 1, where m is odd. Alg. 1 can greatly reduce the simulation time for identifying the worst-case patterns. For instance, the worst-case patterns for an 33-wire bus can be identified by simulating only $5 \times 15 = 75$ transition patterns.

We note that the one assumption about the worst-case patterns for 17-wire buses and the three assumptions about 33-wire buses are made in order to reduce the complexity of finding the worst-case patterns. We did verify our three assumptions about 33-wire buses over 9- and 11-wire buses: the worst cases for all the classes based on Alg. 1 are indeed the worst cases by exhaustive search. This also verifies the assumption for 17-wire buses, since it is one of the three

Algorithm 1 The algorithm for identifying the worst-case pattern, with respect to the three assumptions, in an m -wire bus.

Require: m -wire bus;

Initialize: P_0 is initialized with transitions opposite to wire $\frac{m+1}{2}$, except for wires $\frac{m-1}{2}$, $\frac{m+1}{2}$, and $\frac{m+3}{2}$;

$i = 0$;

repeat

for $j = \frac{m-3}{2}$ to 1 **do**

 Flip the transition of wires j and $(m+1-j)$ in P_i ;

if the delay of wire $\frac{m+1}{2}$ increases **then**

 Keep the changes;

else

 Reverse the changes;

end if

end for

$i = i + 1$;

 Update P_i with the current pattern;

until $P_{i-1} = P_i$

return Worst-case transition pattern for wire $\frac{m+1}{2}$;

assumptions for 33-wire buses. For instance, the worst-case $2C$ pattern of a 11-wire bus is given by $\uparrow\uparrow\uparrow\downarrow\uparrow\downarrow\uparrow\uparrow$ with exhaustive search. In Alg. 1, starting from $\downarrow\downarrow\downarrow\downarrow\uparrow\downarrow\downarrow\downarrow$, the worst-case pattern is found via the order: $\downarrow\downarrow\downarrow\downarrow\uparrow\downarrow\downarrow\downarrow \Rightarrow \downarrow\downarrow\downarrow\uparrow\downarrow\uparrow\downarrow\downarrow \Rightarrow \downarrow\uparrow\uparrow\downarrow\uparrow\downarrow\uparrow\uparrow \Rightarrow \uparrow\uparrow\uparrow\downarrow\uparrow\downarrow\uparrow\uparrow$. Unfortunately, it is difficult to verify Alg. 1, even for one case, for 17- or 33-wire buses, because the complexity would be prohibitive. For instance, for each class focusing on the middle wire, there are $3^{14} = 4782969$ possible patterns for a 17-wire bus (and $3^{30} \doteq 2.06 \times 10^{14}$ for a 33-wire bus), and it takes about 166 days to simulate these cases.

The worst transition patterns for each class in a 33-wire bus, with respect to the three assumptions above, are listed in the second column of Table XII, where the pattern on wires 16, 17, and 18 are shown in the parenthesis. The simulated worst-case delays of wire 17 for all iC patterns, denoted by T_d , are compared with the delays of our five-wire model and the model in [1]. The error percentages of our model and the model in [1] are also shown in Table XII. The **maximum** and **minimum** errors by our model are only 45.23% and 5.95%, respectively, in comparison to 86.87% and 7.61% by the model in [1], respectively. Again, for all classes except $1C$, our five-wire model outperforms the model in [1]. The model in [1] also has a large error percentage for $0C$.

Since our revised models also account for the loading capacitance, we also simulate 17- and 33-wire buses with $C_L = 100$ fF, which represents the loading capacitance induced by a 400 times inverter. The simulated worst-case delays of the middle wire for all iC patterns, denoted by T_d , are compared with the delays T_5^{iC} by our five-wire model as shown in Table XIII. The error percentages of our model are also shown in Table XIII. The worst-case patterns are obtained via Alg. 1. The worst-case patterns are different from those in Tables XI and XII due to the varying of the loading capacitances. However, our five-wire model can still approximate the delays with similar error percentages as those in Tables XI and XII.

Finally, we remark that the longest delays for each class in Tables XI and XII are approximately the same for both 17- and 33-wire buses. Based on the simulation results of 17- and 33-wire buses, we conjecture that our five-wire model would be more accurate than the model in [1] for buses with any number of wires.

C. Performance of CACs

In the simulation results above, we assume the transition patterns are arbitrary. Herein, we assume the transition patterns are limited to those of CACs. We evaluate the performance of our delay model for three families of CACs [12]–[14]: *one Lambda codes* (OLCs), *forbidden pattern codes* (FPCs), and *forbidden overlap codes* (FOCs). Based on our five-wire model, the worst delays of aforementioned CACs are shown in Tables III, IV, and V. Based on the model in [1], the worst delays of aforementioned CACs are approximated by $(1+\lambda)\tau_0$, $(1+2\lambda)\tau_0$, and $(1+3\lambda)\tau_0$, respectively. Since the number of transition patterns is a quadratic function of the number of codewords, it is time-consuming to simulate a large bus to get the worst-case delays on all wires. Hence, for each CAC, we

TABLE XIV

COMPARISON OF SIMULATED DELAYS AND DELAYS GIVEN BY OUR FIVE-WIRE MODEL AND [1] FOR ALL WIRE IN AN 8-WIRE BUS, WHERE T_5^{iC} , T_{b1}^{iC} , AND T_{b2}^{iC} DENOTE THE DELAYS OF WIRES 3-8, WIRE 1 (m), AND WIRE 2 ($m-1$), RESPECTIVELY. ALL THE DELAYS ARE IN ps.

wire i	Delays		
	OLC	FPC	FOC
1	55.36	107.43	107.73
2	32.20	102.71	159.65
3	51.40	106.65	154.59
4	51.06	101.91	162.61
5	50.79	101.89	162.77
6	51.39	106.53	154.62
7	32.46	102.72	160.61
8	55.36	107.39	108.88
[6]	73.50	141.45	209.40
T_5^{iC}	62.09	106.43	152.24
T_{b1}^{iC}	53.43	98.76	98.76
T_{b2}^{iC}	42.52	102.84	157.64

simulate an 8-wire bus. The numbers of codewords of OLC, FPC, and FOC are given by 16, 68, and 149, respectively. The total numbers of transition patterns for OLC, FPC, and FOC are given by 240, 4556, and 22052, respectively. We obtain by simulation the maximum delays of each wire for all transition patterns. The simulation results are shown in Table XIV, where the delays given by our five-wire model and the model in [1] are also included. Intuitively, the worst-case delays of any two symmetric wires are the same, since the symmetric transition of a valid transition pattern is also valid. As shown in Table XIV, the simulated delays of symmetric wires are very close. For OLCs, FPCs, and FOCs, the largest delays are emphasized in boldface. As Table XIV shows, our delay models are more accurate than the model in [1] for all three families of CACs.

IV. CONCLUSIONS AND FUTURE WORK

In this paper, we propose improved analytical delay models for coupled interconnects. We first derive closed-form expressions of the signals on the bus, based on the distributed RC model, and then approximate the delays of different patterns by evaluating these closed-form expressions. We focus on three-wire and five-wire models, and simulation results show that our model has better accuracy than the model in [1]. Although our models are based on three-wire and five-wire buses, they are not limited to these two cases. For a bus with more than five wires, our five-wire model can still approximate delays better than the model in [1].

REFERENCES

- [1] P. P. Sotiriadis and A. Chandrakasan, "Reducing bus delay in submicron technology using coding," *Proceedings of the Asia and South Pacific Design Automation Conference*, pp. 109–114, 2001.
- [2] [Online], available at <http://www.itrs.net/Links/2009ITRS/Home2009.htm>.
- [3] R. Kay and L. Pileggi, "PRIMO: Probability interpretation of moments for delay calculation," *Proceedings of the 35th annual Design Automation Conference*, vol. 35, pp. 463–468, 1998.
- [4] L. Pileggi, "Timing metrics for physical design of deep submicron technologies," *Proc. of International Symposium on Physical Design*, pp. 28–33, April 1998.

- [5] C. J. Alpert, A. Devgan, and C. V. Kashyap, "RC delay metrics for performance optimization," *IEEE Transactions on Computer Aided Design Integrated Circuits System*, vol. 20, no. 5, pp. 571–582, 2001.
- [6] P. P. Sotiriadis, "Interconnect modeling and optimization in deep sub-micron technologies," Ph.D. Dissertation, Massachusetts Institute of Technology, 2002.
- [7] F. Liu, C. Kashyap, and C. J. Alpert, "A delay metric for RC circuits based on the weibull distribution," *Proc. IEEE/ACM International Conference on Computer-Aided Design*, pp. 620–624, 2002.
- [8] J. A. Davis and J. D. Meindl, "Compact distributed RLC interconnect models-part II: Coupled line transient expressions and peak crosstalk in multilevel networks," *IEEE Transactions on Electron Devices*, vol. 47, no. 11, pp. 2078–2087, November 2000.
- [9] A. I. Abou-Seido, B. Nowak, and C. Chu, "Fitted Elmore delay: A simple and accurate interconnect delay model," *Proceedings of IEEE International Conference on Computer Design*, pp. 422–428, April 2002.
- [10] S. Tu, Y. Chang, and J. Jou, "RLC coupling-aware simulation and on-chip bus encoding for delay reduction," *IEEE Transactions on Computer Aided Design Integrated Circuits System*, vol. 25, no. 10, pp. 2258–2264, 2006.
- [11] F. Moll, J. Figueras, and A. Rubio, "Data dependence of delay distribution for a planar bus," *18-th International Workshop, PATMOS 2008*, pp. 409–418, 2008.
- [12] C. Duan, A. Tirumala, and S. Khatri, "Analysis and avoidance of cross-talk in on-chip buses," *The Ninth Symposium on High Performance Interconnects (HOTI '01)*, pp. 133–138, 2001.
- [13] B. Victor and K. Keutzer, "Bus encoding to prevent crosstalk delay," *Proc. IEEE/ACM International Conference on Computer-Aided Design*, pp. 57–63, 2001.
- [14] S. Sridhara, A. Ahmed, and N. Shanbhag, "Coding for reliable on-chip buses: A class of fundamental bounds and practical codes," *IEEE Transactions on Computer Aided Design Integrated Circuits System*, vol. 26, no. 5, pp. 977–982, May 2007.
- [15] X. Wu, Z. Yan, and Y. Xie, "Two-dimensional crosstalk avoidance codes," in *Proc. IEEE Workshop on Signal Processing Systems (SiPS)*, pp. 106–111, October 2008.
- [16] P. P. Sotiriadis and A. P. Chandrakasan, "A bus energy model for deep submicron technology," *IEEE Trans. VLSI Systems*, vol. 10, no. 3, pp. 341–350, 2002.
- [17] C. Duan and S. Khatri, "Exploiting crosstalk to speed up on-chip buses," *Proceedings of the Conference on Design Automation and Test in Europe*, vol. 2, pp. 16–20, February 2004.
- [18] W. C. Elmore, "The transient response of damped linear networks with particular regard to wideband amplifier," *Journal of Applied Physics*, vol. 19, pp. 55–63, January 1948.
- [19] R. Gupta, B. Tutuianu, and L. T. Pileggi, "The Elmore delay as a bound for RC trees with generalized input signals," *IEEE Transactions on CAD*, vol. 16, no. 1, pp. 95–104, January 1997.
- [20] C. Tsai, J. Wu, T. Lee, and R. Hsiao, "Propagation delay minimization on RLC-based bus with repeater insertion," *Proceedings of IEEE Asia-Pacific Conference on Circuits and Systems*, pp. 1285–1288, 2006.
- [21] [Online], "Gigabit repeaters," available at http://focus.ti.com/download/aap/pdf/Gigabit_Repeaters.pdf.
- [22] Y. I. Ismail, E. G. Friedman, and J. L. Neves, "Figures of merit to characterize the importance of on-chip inductance," *IEEE Trans. VLSI Systems*, vol. 7, no. 4, pp. 440–449, December 1999.
- [23] A. Courtay, O. Sentieys, J. Laurent, and N. Julien, "High-level interconnect delay and power estimation," *Journal of Low Power Electronics*, vol. 4, no. 1, pp. 21–33, 2008.
- [24] L. Zhang, J. M. Wilson, R. Bashirullah, L. Luo, J. Xu, and P. D. Franzon, "A 32-Gb/s on-chip bus with driver pre-emphasis signaling," *IEEE Trans. VLSI Systems*, vol. 17, no. 9, pp. 1267–1274, September 2009.
- [25] J. M. Rabaey, *Digital integrated circuits*. Prentice-Hall, 1996.
- [26] T. Sakurai, "Closed-form expressions for interconnection delay, coupling, and crosstalk in VLSI's," *IEEE Transactions on Electron Devices*, vol. 40, no. 1, pp. 118–124, January 1993.
- [27] A. B. Kahng, S. Muddu, and D. Vidhani, "Noise and delay uncertainty studies for coupled RC interconnects," *Proceedings of 12th Annual IEEE International ASIC/SOC Conference*, pp. 3–8, September 1999.
- [28] F. Awwad, M. Nekili, V. Ramachandran, and M. Sawan, "On modeling of parallel repeater-insertion methodologies for soc interconnects," *Circuits and Systems I: Regular Papers, IEEE Transactions on*, vol. 55, no. 1, pp. 322–335, 2008.
- [29] [Online], "PDK for the 45nm technology," available at <http://www.eda.ncsu.edu/wiki/FreePDK>.
- [30] —, "Predictive technology model (PTM)," available at <http://ptm.asu.edu>.
- [31] F. Shi, X. Wu, and Z. Yan, "Improved crosstalk avoidance codes based on a novel pattern classification," in *Proc. IEEE Workshop on Signal Processing Systems (SiPS)*, pp. 245–250, October 2011.
- [32] —, "New crosstalk avoidance codes based on a novel pattern classification," 2012, submitted to *IEEE Transactions on Very Large Scale Integration (VLSI) Systems*.